Protoplasma (2024) 261:333–349
https://doi.org/10.1007/s00709-023-01898-8

ORIGINAL ARTICLE

Comparative immunohistochemical analysis suggests a conserved role of EPS8L1 in epidermal and hair follicle barriers of mammals

Lorenzo Alibardi[1,2] · Marta Surbek[3] · Leopold Eckhart[3]

Received: 19 June 2023 / Accepted: 2 October 2023 / Published online: 27 October 2023

Abstract

The mammalian skin and its appendages depend on tightly coordinated differentiation of epithelial cells. Epidermal growth factor receptor (EGFR) pathway substrate 8 (EPS8) like 1 (EPS8L1) is enriched in the epidermis among human tissues and has also been detected in the epidermis of lizards. Here, we show by the analysis of single-cell RNA-sequencing data that EPS8L1 mRNA is co-expressed with filaggrin and loricrin in terminally differentiated human epidermal keratinocytes. Comparative genomics indicated that *EPS8L1* is conserved in all main clades of mammals, whereas the orthologous gene has been lost in birds. Using a polyclonal antibody against EPS8L1, we performed an immunohistochemical screening of skin from diverse mammalian species and immuno-electron microscopy of human skin. EPS8L1 was detected predominantly in the granular layer of the epidermis in monotremes, marsupial, and placental mammals. The labeling was partly associated with cell membranes, and it was evident along the perimeter of keratinocytes at the transition with the cornified layer of the epidermis, similar to involucrin distribution. Basal, spinous, and the fully mature cornified layers lacked immunolabeling of EPS8L1. In addition to the epidermis, the hair follicle inner root sheath (IRS) was immunolabeled. Both epidermal granular layer and IRS contribute to the barrier function of the skin, suggesting that EPS8L1 is involved in the regulation of these barriers.

Keywords Epidermis · Keratinocytes · Mammals · Epidermal growth factor receptor · Immunohistochemistry

Introduction

The mammalian epidermis forms an efficient barrier against water loss from the inside and against the entry of chemicals and microbes from the outside of the skin (Sokolov 1982; Elias and Choi 2005; Eckhart and Zeeuwen 2018; Sachslehner et al. 2023). This barrier resides in the two outermost layers of the epidermis, the cornified layer (stratum corneum), and the granular layer. The latter is characterized by the expression of filaggrin and loricrin, the formation of keratohyalin granules that are seen in histological sections, and by the presence of tight junctions which limit intercellular diffusion (Steven et al. 1990; Kalinin et al. 2002; Matsui and Amagai 2015; Ishida-Yamamoto et al. 2018). The secretion of lipids into the intercellular space of the stratum corneum, the cross-linking of proteins encoded by genes of the epidermal differentiation complex (EDC) and others, and the dynamic remodeling of cell junctions during terminal differentiation of keratinocytes are critical for the maintenance and continuous regeneration of the epidermal barrier (Menon et al. 1992; Rawlings et al. 1994; Kalinin et al. 2002; Gorzelanny et al. 2020). Many proteins have been implicated in the regulation of the skin barrier, including epidermal growth factor (EGF) and its receptor (EGFR) (Rübsam et al. 2017), but the functions of several proteins present in the granular and cornified layers of the epidermis are unknown.

EGFR pathway substrate 8 (EPS8) like 1 (EPS8L1) mRNA was identified as a skin-enriched gene transcripts and EPS8L1 protein was detected in the granular layer of human epidermis (Edqvist et al., 2015). The EPS8L1 protein shares the domain organization with EPS8, which is involved in Ras signaling and actin remodeling (Tocchetti

Handling Editor: Reimer Stick

✉ Lorenzo Alibardi
lorenzo.alibardi@unibo.it

[1] Comparative Histolab Padova, Padua, Italy

[2] Department of Biology, Via Selmi 3, University of Bologna, 40126 Bologna, Italy

[3] Department of Dermatology, Medical University of Vienna, Vienna, Austria

et al. 2003; Offenhauser et al. 2004), and two further EPS8-like proteins (EPS8L2, EPS8L3). At the amino acid sequence level EPS8L1 is 38.5% identical to EPS8, suggesting that their functions are similar. As EPS8 was originally characterized as a component of EGFR signaling (Lanzetti et al. 2000), the specific expression of EPS8L1 in the epidermis suggests that EPS8L1 might be involved in cutaneous EGFR signaling, which is critical for growth and differentiation of epidermal keratinocytes (Lichtenberger et al. 2013; Rübsam et al. 2017; Amberg et al. 2019; Barresi et al. 2022; Green et al. 2022). However, like EPS8 (Frittoli et al. 2011; Giampietro et al. 2015), EPS8L1 may also play EGFR-independent roles.

Based on its identification as skin-enriched gene, we hypothesized that EPS8L1 is associated with skin-specific structures or functions and determined the expression pattern and protein localization of EPS8L1 in the skin of phylogenetically diverse species representing the entire class of mammals, including monotremes, marsupials, and placentals. Our data extend the knowledge about EPS8L1 expression beyond human epidermis and suggest an evolutionarily conserved role of EPS8L1 in the regulation of the mammalian epidermal barriers.

Materials and methods

Comparative gene analysis

Genes orthologous to human *EPS8L1* were identified in the genome sequences of vertebrates according to a previously described approach (Eckhart et al. 2006). The sequences were obtained from GenBank at the National Center for Biotechnology Information (NCBI), https://www.ncbi.nlm.nih.gov/genbank/, last accessed on 7 June 2023). Orthology was confirmed by reciprocal BLAST searches and detection of shared synteny.

Analysis of single-cell RNA-sequencing (scRNA-seq) data

scRNA-seq data from human hip skin were downloaded from GenBank (accession number GSM5410886) and analyzed, as described previously (Kalinina et al. 2021). Uniform manifold approximation and projection (UMAP) plots were generated to achieve dimension reduction and facilitate the identification of cell clusters. mRNA expression levels were diplayed as color intensity for each cell.

Skin samples

The skin samples and the related permits were collected in previous studies (see below), and the embedded tissues have been re-sectioned to be utilized in the present study. Skin from different regions of the monotremes platypus (*Ornithorynchus anatinus*, foot-web skin) and echidna (*Tachyglossus aculeatus*, ventral skin), the marsupials red kangaroo (*Osphrantus rufus*, dorsal skin), wombat (*Vombatus ursinus*, dorsal skin), brush-tail possum (*Trichurus vulpecula*, ventral and ear skin), striped-face dunnart (*Sminthopsis macroura*, belly skin) and the placentals mole (*Talpa europaea*, ventral skin), bat (*Pipistrellus kuhnii*, alar skin), mouse (*Mus musculus*, newborn and adult dorsal skin), newborn rat (*Rattus norvegicus*, tail and dorsal skin), rabbit (*Oryctolagus cuniculus*, ear skin), hamster (*Mesocricetus auratus*, newborn dorsal skin), cat (*Felis domestica*, belly skin), and human (*Homo sapiens*, scalp and finger skin) were here utilized (Alibardi 2004a,b, 2006, 2010, 2012; Alibardi and Maderson, 2004; Alibardi et al. 2005). Human skin from the scalp and digit was provided by the consent information of two adult individuals, as previously reported (Alibardi et al. 2004).

Preparation of samples

Briefly, after fixation in Carnoy or 4% paraformaldehyde in neutral phosphate buffer 0.1 M for about 8 h at 4 °C, the small skin tissues (2–4 mm) were dehydrated and embedded at 0–4 °C under UV in Lowcryl or Bioacryl resins for 2–3 days (Scala et al. 1992). The samples were sectioned at 2–4 µm in thickness using an ultramicrotome, and they were collected on glass slides for staining (1% toluidine blue) or immunofluorescence analysis.

Immunofluorescence analysis

Immunofluorescence was carried out using a rabbit polyclonal antibody raised against the amino acid residues 384–469 of human EPS8L1 (HPA041851, Sigma, USA). After 1 h pre-incubation in buffer with 2% normal goat serum at room temperature, the sections were exposed to the primary antibody (dilution 1:200) overnight at 0–4 °C. In control sections, the primary antibody was omitted. Following repeating rinses in the buffer, the sections were incubated with an anti-rabbit immunoglobulin FITC-conjugated secondary antibody, diluted 1:200 v/v, for 70 min at room temperature. As nuclear counterstaining for the green signal of FITC, propidium iodide (PI, red) was utilized at a dilution of 1:1000 in buffer. The sections were stained with PI for 10 min in the dark at room temperature. After mounting the sections with Fluoromount (Sigma), they were observed under a fluorescence microscope (Euromex Microscopen B.V., Novex B Fluo, Holland) equipped with a fluorescein

filter (FITC, Green filter, G) and images were recorded by a digital camera (Toupcam, Labwaretools, version 3.7, Treviso, Italy).

Immunogold electron microscopy

From the two human skin samples, thin sections were collected using an ultramicrotome on nickel grids, and they were immunostained using gold particles of 10 nm in diameter (Sigma). The sections were pre-incubated for 10 min at room temperature in 0.05 M tris(hydroxymethyl)aminomethane (Tris)-HCl buffer at pH 7.6, containing 1% cold water fish gelatin, and then incubated overnight at 0–4 °C in the primary antibody against EPS8L1 and diluted 1:200 v/v in the same buffer. In controls, the primary antibody was omitted. In order to

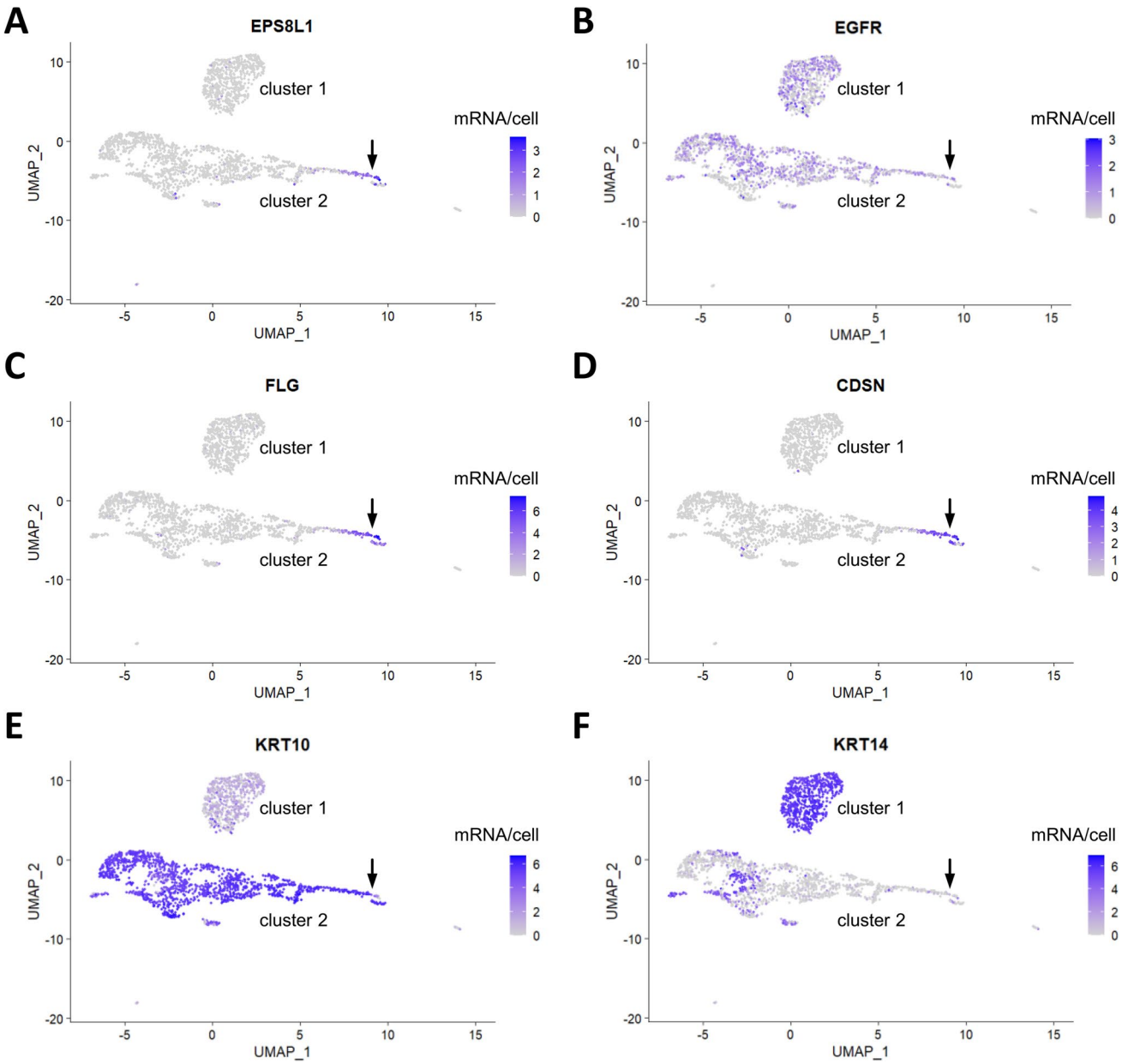

Fig. 1 Identification of *EPS8L1* expression in single-cell RNA-sequencing (scRNA-seq) data. Expression levels of *EPS8L1* (**A**), *EGFR* (**B**), *FLG* (**C**), *CDSN* (**D**), *KRT10* (**E**) and *KRT14* (**F**) are indicated in uniform manifold approximation and projection (UMAP) plots of scRNA-seq data from human hip skin. The color intensity of the dots, each corresponding to a cell isolated from the skin, is proportional to the abundance of the respective mRNA. Arrows point to an EPS8L1-expressing subcluster of cells. Clusters 1 and 2 are predicted to represent keratinocytes of the basal and suprabasal epidermal layers, respectively. de, dermis

compare the labeling with that of involucrin and loricrin, also antibodies against the latter proteins were utilized as reported in previous studies (details in Alibardi et al. 2004; Alibardi 2010, 2012). An anti-human involucrin mouse antibody (I-9018, Sigma, USA) was utilized.

The sections on grids were rinsed in Tris buffer and incubated for 1 h at room temperature with anti-rabbit (for EPS8L1) or anti-mouse (involucrin) immunoglobulin 10-nm diameter gold-conjugated secondary antibodies at 1:100 dilution v/v. After the immunoreaction, the grids were rinsed in Tris buffer, distilled water, and dried, stained for 4 min with 2% uranyl acetate, and then observed and photographed under an electron microscope Zeiss 10C/CR operating at 60 kV.

Results

mRNA expression analysis of EPS8L1 in the skin

To determine the expression of human *EPS8L1* mRNA in human skin, we analyzed a set of scRNA-seq data available in the National Center for Biotechnology Information (NCBI) Gene Expression Omnibus (GEO) repository. *EPS8L1* was expressed specifically in a group of cells (Fig. 1A) that also expressed the potential signaling partner EGFR (Fig. 1B), markers of terminal differentiation of keratinocytes such as filaggrin (FLG, Fig. 1C) and corneodesmosin (CDSN, Fig. 1D), and the suprabasal epidermal layer keratin KRT10 (Fig. 1E). EPS8L1 was not expressed in FLG-negative KRT10-positive keratinocytes (Fig. 1C, E, cluster 2) and in KRT14-positive basal keratinocytes (Fig. 1F, cluster 1). This expression pattern was congruent with the immunostaining pattern of EPS8L1 observed in human epidermis (Edqvist et al. 2015), supporting the specificity of the published antibody.

We also investigated transcriptome data from studies in which the granular layer was separated from the less differentiated layers of the epidermis (Gulati et al. 2013; Matsui et al. 2021). *EPS8L1* mRNA was enriched in the granular layer of human and mouse epidermis (Table 1). This enrichment was paralleled by enrichment of known markers of terminal keratinocyte differentiation, such as *FLG2* (Wu et al. 2009) and *HAL* (Eckhart et al. 2008), whereas the marker of the basal epidermis, *KRT14* was downregulated (Table 1). These data showed that *EPS8L1* mRNA expression is associated with terminal differentiation of keratinocytes in human and mouse skin.

Comparative gene and amino acid sequence analysis of EPS8L1

The conservation of the *EPS8L1* gene in a wide range of species was investigated by comparative genomics using genome sequences deposited in NCBI GenBank. *EPS8L1* orthologs were detected in species from all major clades of vertebrates with the exception of birds (Fig. 2A). This distribution of the gene suggests that *EPS8L1* has originated, presumably by duplication of the *EPS8* gene (Tocchetti et al. 2003), in a piscine ancestor of modern vertebrates. *EPS8L1* was lost in birds, whereas orthologous genes have been conserved in non-avian sauropsids such as lizards (Alibardi 2023) and in mammals.

To investigate the localization of EPS8L1 protein in the skin of mammals, we used a polyclonal antibody that was raised against an epitope of human EPS8L1 (Fig. 2B). The amino acid sequence of this epitope was largely conserved in mammalian species with more than 55% sequence identity in echidna and platypus,

Table 1 Conserved upregulation of *EPS8L1* in the granular layer of human and mouse

Gene symbol	Gene name	Human		Mouse	
		FC (granular/basal layer)	*P* value	FC (granular layer/total epidermis)	*P* value
EPS8L1	EPS8 like 1	477.4	8.27E−05	9.6	1.14E−04
FLG2	Filaggrin family member 2	1341.8	8.89E−05	16.2	4.75E−03
HAL	Histidine ammonia-lyase	95.8	2.38E−04	2.9	4.09E−02
KLK7	Kallikrein related peptidase 7	112.1	6.25E−04	4.5	1.41E−02
LCE1B	Late cornified envelope 1B	342.7	2.86E−04	18.0	8.71E−03
KRT14	Keratin 14	0.21	5.66E−04	0.01	4.24E−03

mRNA levels were obtained from data published by Gulati et al. (2013) and Matsui et al. (2021). *P* values indicate the significance of differences between expression levels in granular versus basal layer and in the granular layer versus total epidermis

FC fold change

representing the basal mammalian clade Monotremata (Fig. 2B), suggesting that cross-reactivity of the polyclonal antibody allowed the detection of EPS8L1 in mammalian tissues.

Histology

We used tissue samples that were collected in previous comparative studies of mammalian skin, derived from plastic-embedded skin. To explore the variation in epidermal structures across mammals (Sokolov 1982; Alibardi and Maderson, 2004), we subjected the skin samples to histological analysis by toluidine blue staining.

In the webbed epidermis of the platypus, the epidermis showed extensive and deep papillae but a distinct granular layer (better visible in other skin areas) was not visible or was even absent (parakeratosis; Fig. 3A). The hairy skin of the echidna showed a variable number of spinous layers, 2–3 layers of granular cells and a

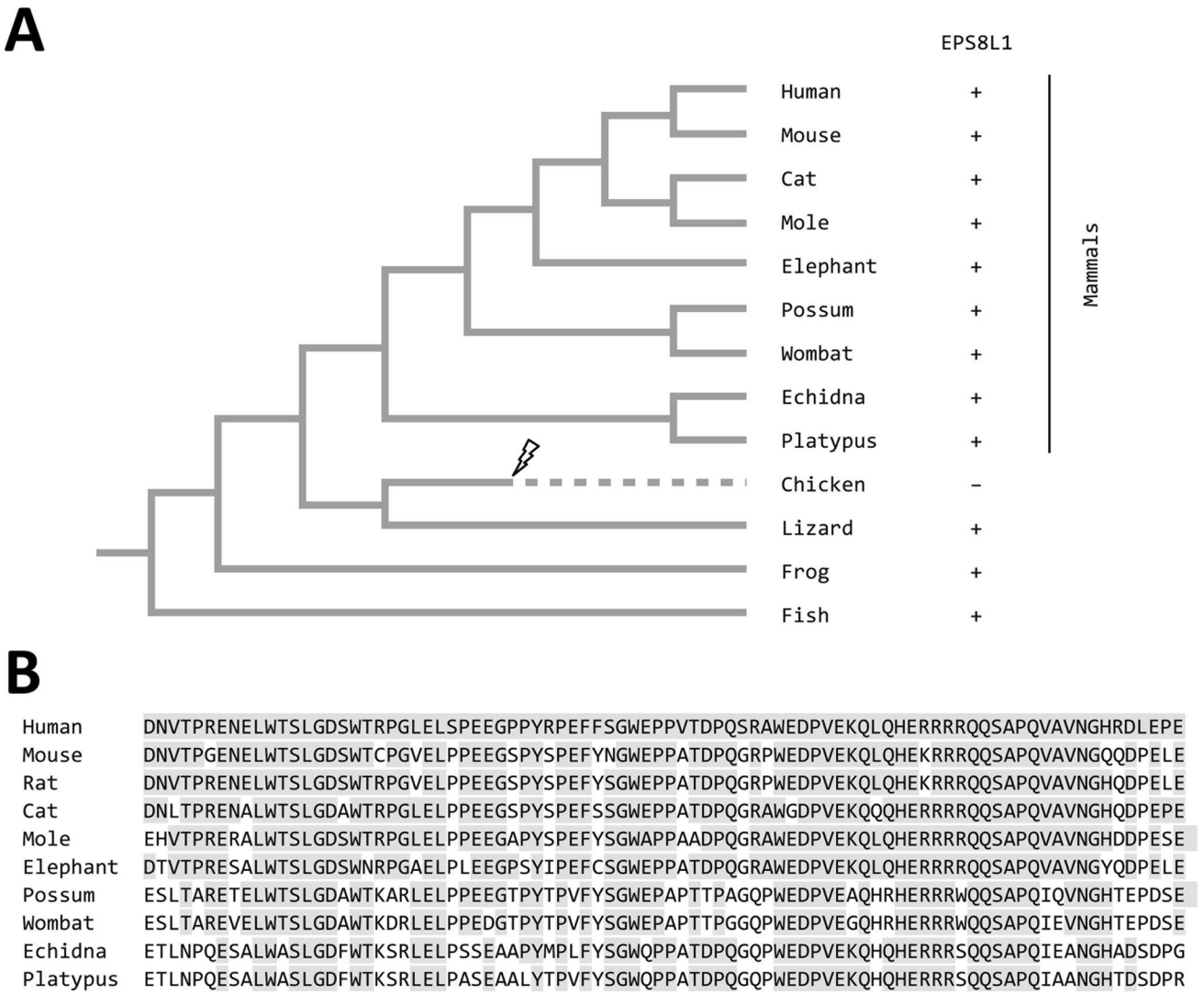

Fig. 2 Evolutionary history of the *EPS8L1* gene and conservation of the EPS8L1 epitope in mammals. **A** Phylogenetic tree of vertebrates indicating presence (+) or absence (−) of an *EPS8L1* gene in representative species. The discontinuous line indicates loss of the *EPS8L1* gene in the evolutionary lineage leading to birds. Besides mammalian species (see below for details), lizard (*Anolis carolinensis*), frog (*Xenopus tropicalis*) and zebrafish (*Danio rerio*) were investigated. **B** Alignment of amino acid sequences homologous to the epitope of the EPS8L1 antibody used in this study. Amino acid residues identical to those of human EPS8L1 are shaded gray. GenBank accession numbers of EPS8L1 proteins: NP_573441.2 (human, *Homo sapiens*), NP_001277345.1 (mouse, *Mus musculus*), NP_001101937.1 (rat, *Rattus norvegicus*), XP_044903226.1 (cat, *Felis catus*), XP_054553361.1 (mole, *Talpa occidentalis*), XP_003406660.3 (elephant, *Loxodonta africana*), XP_036602992.1 (possum, *Trichosurus vulpecula*), XP_027715910.1 (wombat, *Vombatus ursinus*), XP_038608268.1 (echidna, *Tachyglossus aculeatus*), XP_039769217.1 (platypus, *Ornithorhynchus anatinus*)

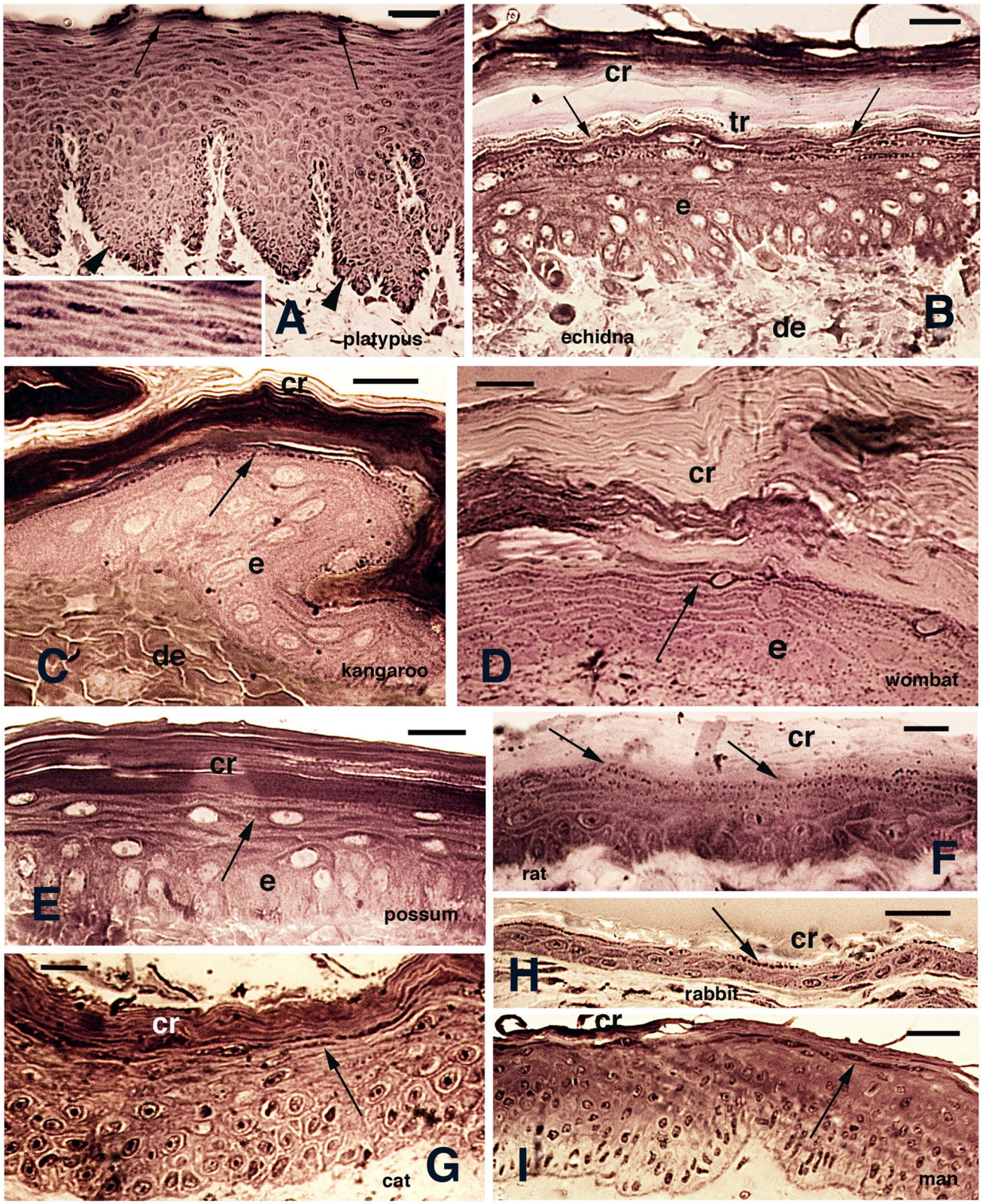
A
platypus
cr
tr
e
de
B
echidna
cr
e
de
C
kangaroo
cr
e
D
wombat
cr
e
E
possum
cr
rat
F
cr
rabbit
H
cr
cat
G
cr
man
I

◂**Fig. 3** Histology of the epidermis in various mammals. Toluidine blue stain. Scale bar, 20 µm in **A**, **G**, **H**, and **I**; scale bar, 10 µm in **B**, **C**, **D**, **E**, and **F. A** Platypus web epidermis (arrows point to the corneous layer) with extended papillae (arrowheads). The inset details the granular content of pre-corneous keratinocytes. **B** Ventral epidermis of echidna with granular layer (arrows) and relatively thick corneous layer. **C** Dorsal epidermis of red kangaroo with granular layer (arrow). **D** Dorsal skin epidermis of wombat with the granular layer (arrow) and a thick corneous layer. **E** Digit epidermis of brushtail possum with granular cells (arrow). **F** Tail epidermis of rat with atratified granular layer (arrows). **G** Ventral epidermis of cat with granular cells (arrows). **H** Ear epidermis of rabbit with thin granular layer (arrow). **I** Scalp human epidermis showing a thin granular layer (arrow). Abbreviations: cr, corneous layer; e, epidermis; tr, transitional layer

fragile and variably thick corneous layer that was often fragmented at sectioning (Fig. 3B). The red kangaroo epidermis was generally very thin and fragile, featuring 2–3 cell layers, while one single granular layer (absent or not visible in some areas) was present in contact with the lower part of the corneous layer that often appeared fragmented (Fig. 2C). The epidermis of the wombat here analyzed (dorsal areas) was multilayered with 1–2 layers of granular cells (Fig. 2D), but the granular layer was not discernible in some samples. The corneous layer often appeared thicker than the viable epidermis. The epidermis of the ear in the possum appeared stratified in some areas, but in other areas, it was much thinner, and a granular layer made of 1–2 cell layers was visible underneath the denser inner part of the corneous layer (Fig. 2E). The outer paler part of the stratum corneum was often desquamating.

Also, placental epidermis varied in thickness and development of the granular layer. In the juvenile rat (2 days post-parturition), the epidermis was thick and 2–3 layers of granular cells were well visible over most of the dorsal skin (Fig. 2F). Likewise, the corneous layer appeared thicker at this stage than in adult epidermis. The ventral epidermis of the cat appeared multilayered and showed a flat granular layer, generally bilayered, and uniformly distributed along the epidermis (Fig. 2G). The flat corneocytes of the corneous layer often appeared distinct. The epidermis of rabbit (like in the mouse, dunnart, bat, and kangaroo) was very thin, comprising a flat to cubic basal layer, an irregularly distributed spinous layer and only in some areas a single granular layer was observed (Fig. 2H). The corneous layer was very thin and fragile in the ventral area (thicker in the ear) and often appeared artifactually separated from the viable epidermis. Finally, the human scalp epidermis here examined showed the typical stratification with one, sometimes two flat granular layer cells and a thin corneous layer with desquamating cells (Fig. 2I).

Immunofluorescence analysis of EPS8L1 in the epidermis of mammals

EPS8L1 was detected by immunofluorescence analysis in the epidermis of monotremes (Fig. 4A–F), marsupials (Figs.4G-I, 5A-F) and placental mammals (Fig. 5H-J, Fig. 6). The epidermis of the platypus, a monotreme, showed a weak but specific immunolabeling for EPS8L1 in the corneous layers, but the immunofluorescence faded in the more external layers (green fluorescence in Fig. 4A, B). In control sections, the corneous layer was not labeled or displayed a weak and yellowish autofluorescence in some regions (Fig. 4C). The lower part of the corneous layer of echidna was unevenly immunolabeled, but this was probably due to the difficulty to obtain a uniformly sectioned corneous layer (Fig. 4E, D). Control sections appeared unlabeled (Fig. 4F).

The epidermis of the possum, a marsupial, showed a specific EPS8L1 labeling in the granular and transitional (low corneous) layers (Fig. 4G). The examination at higher magnification showed a more intense labeling along the perimeter of coneocytes (Fig. 4H) which was very weak or absent in control sections (Fig. 4I). The thin epidermis (dorsal) of the kangaroo evidenced an immunofluorescent corneous layer, especially in its lowermost region (Fig. 5A). Despite the fragmentation in numerous areas of the epidermis, where the distinction of a granular layer was difficult, the linear fluorescence indicated that the more intensely labeled part of the epidermis corresponds to the granular layer and the lower part of the corneous layer (Fig. 5B). A low and yellowish fluorescence sometime appeared in controls (Fig. 5C). The multilayered epidermis of the wombat appeared poorly reactive and unevenly labeled in some spots of the thick corneous layer, with not much difference to the negative control sections (Fig. 5D, E). Finally, the very thin epidermis of the dunnart showed labeling in the thin and often fragmented corneous layer. However, although some labeled granular material was sometimes seen, it was difficult to detect a granular layer with the employed method (Fig. 5F). As seen in histology the thin external corneous layers were often lost with sectioning (like in mouse, rabbit. and bat).

The epidermis of the newborn mouse (1 day post-delivery) was stratified and showed immunolabeling in the upper, granular layers while the labeling faded in

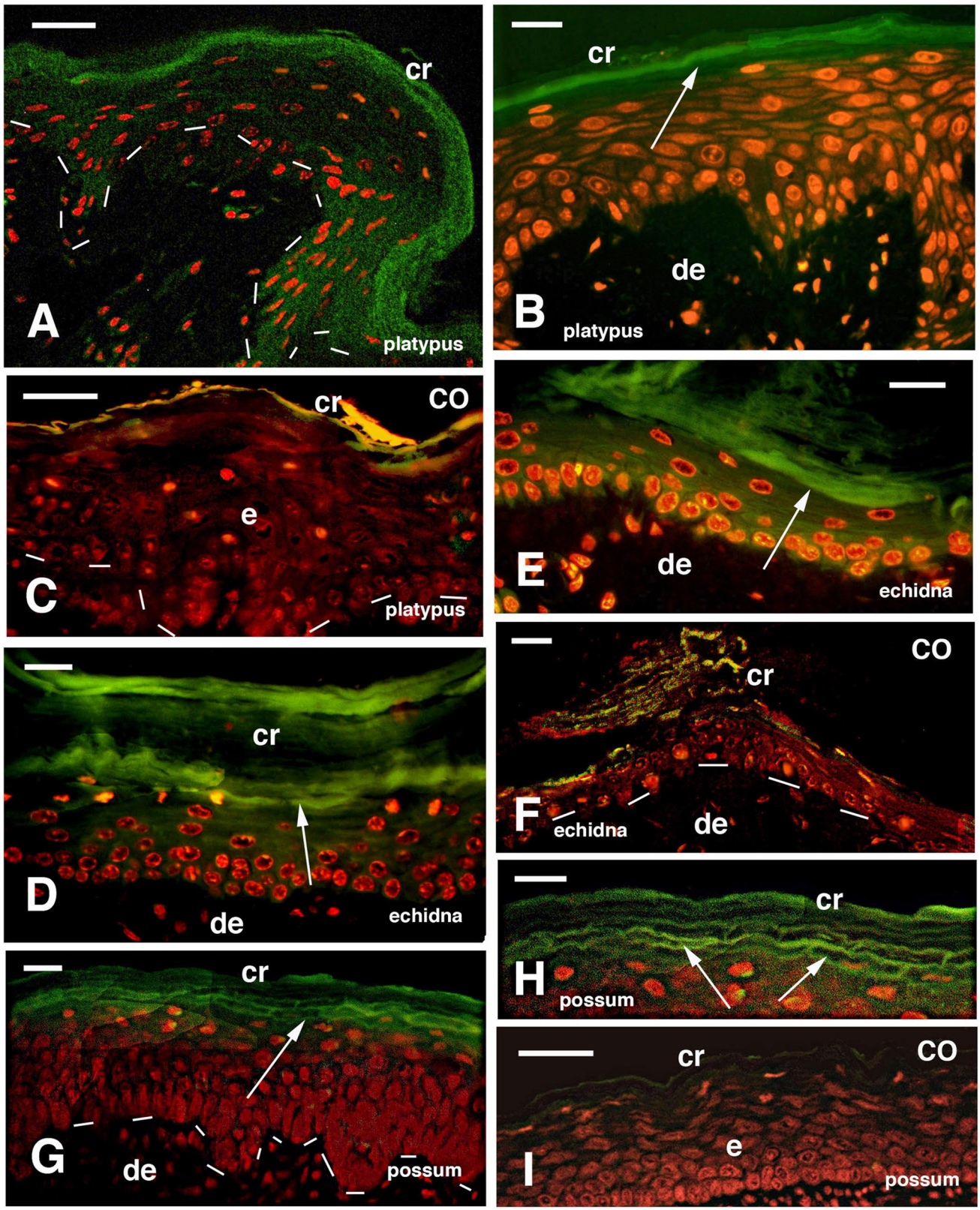
A
cr
platypus
B
cr
de
platypus
C
cr
CO
e
platypus
D
cr
de
echidna
E
de
echidna
F
CO
cr
echidna
de
G
cr
de
possum
H
cr
possum
I
cr
CO
e
possum

◂**Fig. 4** Immunofluorescence in the epidermis of monotremes and marsupials (green fluorescence for EPS8L1; red fluorescence for propidium iodide). Scale bar, 20 µm in **A**, **C**, **and I**; scale bar, 10 µm in **B**, **D**, **E**, **F**, **G**, and **H**. **A** Platypus skin with immunolabeled maturing corneous layer. **B** Hairy tail epidermis of platypus with immunolabeled granular-transitional layer (arrow). **C** Control platypus epidermis. **D** Echidna dorsal epidermis. The arrow indicates the transitional layer. **E** Ventral epidermis of echidna with transitional layer (arrow). **F** Immunonegative control epidermis of echidna. **G** Ear epidermis of brush tail possum. Arrows indicate the immunofluorescent granular/transitional layer. **H** Close view of transitional layer cells with the intense immunofluorescence along their perimeter (arrow). **I** Immunonegative control section of possum epidermis. Abbreviations: cr, corneous layer; de, dermis; e, epidermis. Dashes underline the epidermis

the desquamating external layers of newborn epidermis (Fig. 5G). The adult mouse epidermis only showed a very thin immunolabeled corneous layer, and no distinction of the granular layer was evident in this thin epidermis (Fig. 5H). The external layers of the mouse epidermis were flaking and unlabeled. The wing or pectoral skin of the bat appears folded and a very thin corneous layer appeared immunolabeled, but no distinction of the granular and corneous layers was possible in immunofluorescence (Fig. 5I). Also, for the bat epidermis, fragments of likely external corneocytes appeared unlabeled. The epidermis of the newborn rat showed a thickened granular layer that appeared immunofluorescent, like the lowermost part of the corneous layer while flaking external

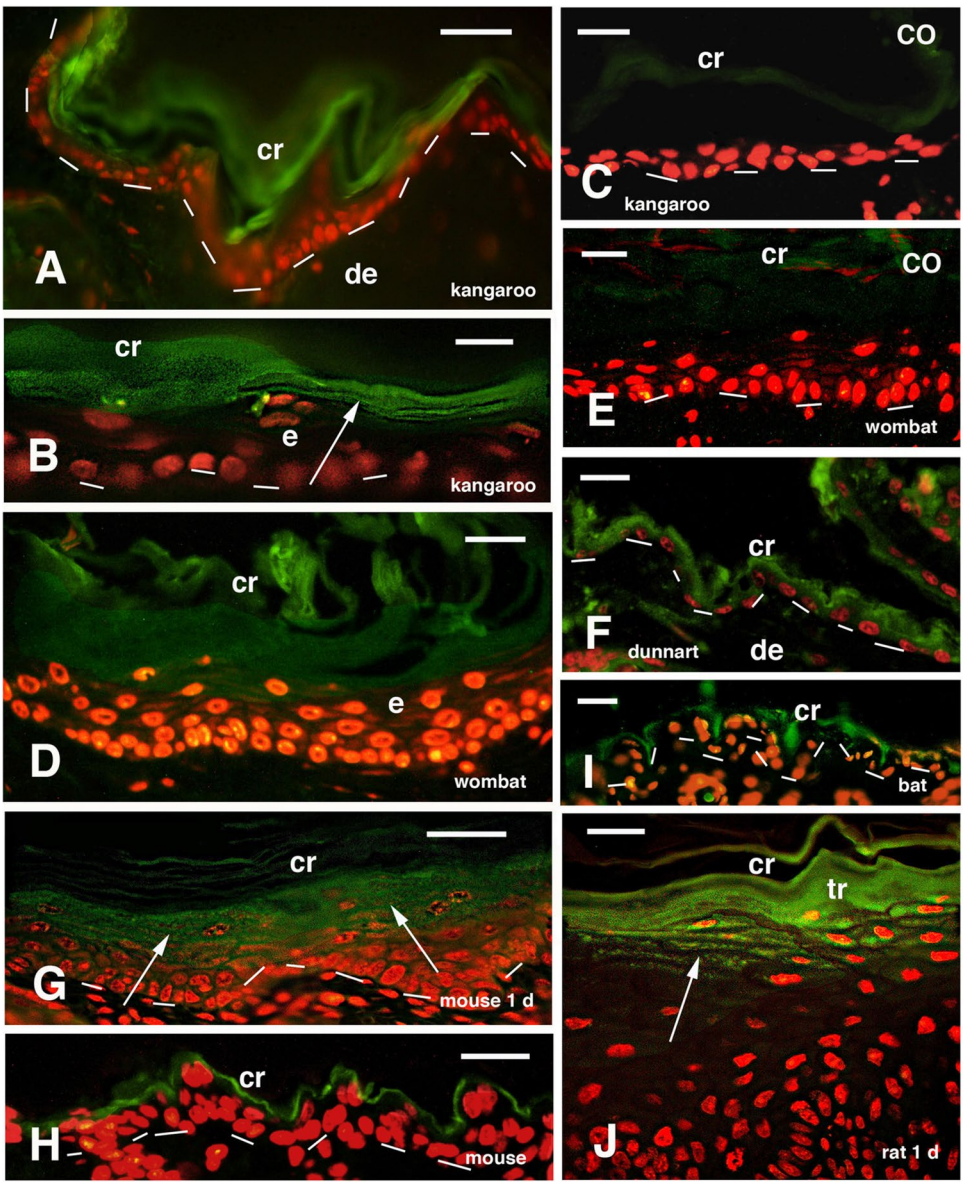

Fig. 5 Immunofluorescence in the epidermis in marsupial and placentals (green fluorescence for EPS8L1, red fluorescence for propidium iodide). Scale bar, 20 µm in **A** and **G**; scale bar, 10 µm in **B**, **C**, **D**, **E**, **F**, **H**, **I**, and **J**. **A** Kangaroo epidermis with immunofluorescent transitional-corneous layer. **B** Other epidermal region of kangaroo skin with labeling in the thin granular layer (arrow). **C** Immunonegative section of kangaroo epidermis. **D** Wombat epidermis with flebile labeling in upper pre-corneous and corneous layer. **E** Immunonegative section of wonbat epidermis. **F** Thin epidermis of dunnart with immunofluorescent corneous layer. **G** Mouse newborn epidermis with immunofluoreswcent pre-corneous layers (arrows). **H** Adult mouse epidermis with thin pre-corneous layer (most corneous layer has been lost in sectioning). **I** Thin bat epidermis with immunofluorescence in the corneous layer (most is lost with sectioning). **J** Newborn rat epidermis with multilayered stratified granular cells (arrow). Abbreviations: cr, corneous layer; de, dermis; tr, transitional layer. Dashes underline the epidermis

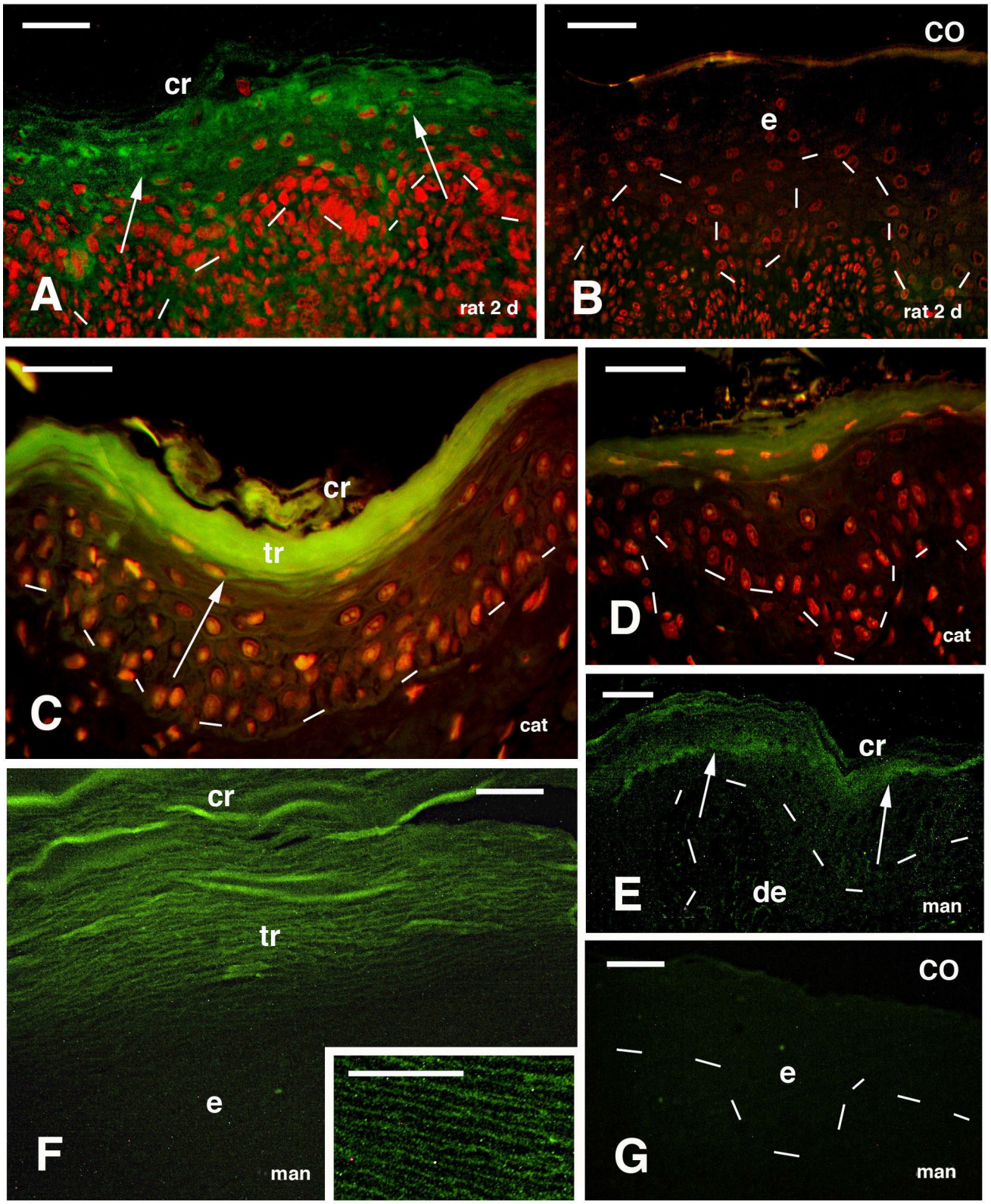
cr
A
rat 2 d
CO
e
B
rat 2 d
cr
tr
C
cat
D
cat
cr
E
de
man
cr
tr
e
F
man
CO
e
G
man

◂**Fig. 6** Immunofluorescence in the epidermis in placentals, including man (green fluorescence for EPS8L1; red fluorescence for propidium iodide). Scale bar, 20 µm in **A**, **B**, **C**, and **D**; scale bar, 10 µm in **E**, **F**, and **G**. **A** Newborn adult rat epidermis with immunolabeled granular-transitional layers (arrows). **B** Negative control section of rat epidermis. **C** Ventral cat epidermis with intensely labeled granular and transitional layers (arrow). **D** Cat control epidermis with weakly stained (autofluorescent) transitional layer. **E** Immunolabeled human scalp epidermis. Arrows indicate the immunolabeled granular layer. **F** Detail of thick corneous layer in human finger epidermis. The transition layer is composed of elongated corneocytes with immunofluorescence perimeter. The inset at higher magnification evidences the perimetral immunolabeling of transitional corneocytes. **G** Immunonegative epidermal section. Abbreviations: cr, corneous layer; de, dermis; e, epidermis; tr, transitional layer. Dashes underline the epidermis

corneocytes were unlabeled (Figs. 5J, 6A). Control sections were unlabeled and a variable yellowish fluorescence was observed (Fig. 6B). Also, the epidermis from cat showed a more intense labeling in the granular but especially in the lower part of the corneous layer (transitional/non-completely mature) while the immunofluorescence faded and disappeared in the flaking external corneocytes (Fig. 6C). The transitional layer of cat sections appeared unlabeled or weakly autofluorescent in control sections (Fig. 6D). The human epidermis showed immunolabeling mainly located along the granular layer and in the lowermost part of the corneous layer, while the immunofluorescence was lost in external and desquamating corneocytes (Fig. 6E). In corneocytes of human epidermis, the labeling appeared more concentrated along the plasma membrane, as it was well seen in regions with a thick corneous layer (finger; Fig. 6F and inset). Control sections were negative or showed a weak fluorescence in the outer stratum corneum (Fig. 6G).

Immunohistochemical detection of EPS8L1 in hair follicles

Immunofluorescence observations were conducted only in few species with clearly visible and differentiating cells of the inner root sheath (IRS) in the platypus, wombat, mole, and hamster. Hairs in platypus were intensely immunolabeled in the IRS, while the fluorescence was less intense in the cuticle and the cortex of the hair fiber but showed a patchy labeling, the latter likely present in sparse cells of the medulla (Fig. 7A). Control sections showed that the cuticle was partially autofluorescent, so its fluorescence is partially or mainly non-specific (Fig. 7B). A less intense but immune-specific fluorescence is present also in the cornifying layers of the outer root sheath (ORS). The large wombat hairs, cut at low levels of the follicle, contained numerous nuclei of differentiating cortical cells and one layer of cuboidal cuticle cells that were surrounded by a corona of green immunolabeled cells of the IRS (Fig. 7C). The differentiating cells of the Henle layer contained large trichohyalin-labeled granules, also present but generally smaller in the Huxley layer (Fig. 7D). Also, in mole and hamster hairs, the IRS appeared the more intense immunolabeled for EPS8L1 (not shown). Control sections appeared immune-negative (Fig. 7E).

Immunogold labeling of human epidermis for EPS8L1 and involucrin

The observations under the electron microscope in both samples of human epidermis showed a weak but specific immunolabeling pattern, reflecting the localization observed in immunofluorescence. Sparse gold particles were detected only in the granular and transitional layers, and they were localized in the cytoplasm among keratin filaments or/and also associated with dense aggregations of corneous material, the dense component of keratohyalin and associated keratin bundles (Fig. 8A). A diffuse but localized labeling was also detected along the desmosomes of keratinocytes in the pre-corneous region (Fig. 8B–D). Scattered immuno-gold particles were seen in the cytoplasm of corneocytes localized in the lowermost part of the stratum corneum and transitional, often associated to keratin bundles. Interestingly, the F-granules component of keratohyalin with a reticulated pattern, were unlabeled (Fig. 8C). Basal keratinocytes, those of the spinous layers, and fully mature corneocytes of external corneous layer were unlabeled for EPS8L1, aside from rare sparse gold particles at random. In control sections, rare or no gold particles were detected (Fig. 8E).

The observation of the immunogold labeling for involucrin showed a more intense labeling than using the EPS8L1 antibody, especially associated with keratin bundles of keratinocytes of the upper spinous and granular layer, but no labeling was detected on keratohyalin granules (Fig. 9A). The gold immunolabeling remained evenly distributed over the pre-corneous and corneous keratinocytes, although it tended to decorate especially along the cell corneous envelope of mature corneocytes (Fig. 9B). No labeling was instead observed in control sections (Fig. 9C).

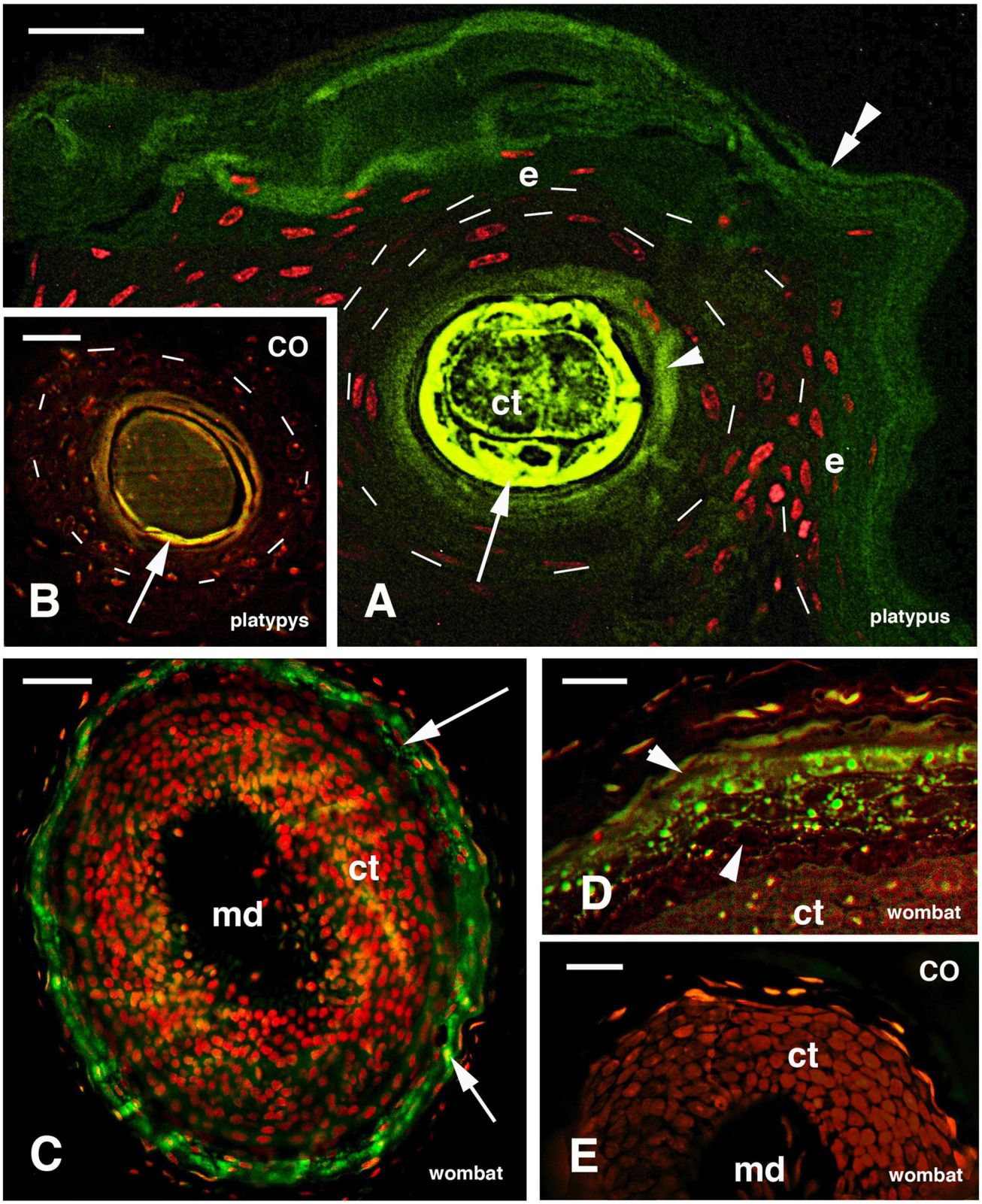
e
co
ct
e
B
platypys
A
platypus
ct
md
C
wombat
D
ct
wombat
co
ct
E
md
wombat

◂**Fig. 7** Immunofluorescence of hairs in platypus (**A** and **B**) and wombat (**B**, **C**, **D**, and **E**), evidencing the IRS (green fluorescence for EPS8L1; red fluorescence for propidium iodide). Scale bar, 20 µm in **A**, **B**, and **C**; scale bar, 10 µm in **D** and **E**. **A** Skin section including a cross-sectioned hair with intensely labeled IRS (arrow). The arrowhead points to the cornifying ORS, while the double arrowhead indicates the cornifying epidermal layer. **B** Control section showing autofluorescence in the hair cuticle (arrow). **C** Cross-sectioned hair with labeled IRS (arrows). **D** Detail of the IRS (arrowheads) showing the immunolabeled trichohyalin granules of variable size. **E** Immunonegative control section (co). Abbreviations: ct, cortex; e, epidermis; md, medulla. Dashes underline the epidermis/ORS

Discussion

Members of the EPS8 protein family differ in their expression pattern and have been implicated in different biological processes. EPS8L1 is unique with regard to its predominant expression in the skin (Edqvist et al., 2015), whereas EPS8 and EPS8L2 have a broad tissue expression pattern, and EPS8L3 is enriched in the gut. Mutations of EPS8 and EPS8L2 lead to hearing loss (Zampini et al. 2011; Furness et al. 2013), which was attributed to an essential role of EPS8 for the elongation of stereocilia and a requirement of of EPS8L2 for maintenance of stereocilia (Zampini et al. 2011; Furness et al. 2013). Mutations of EPS8L3 were linked with hypotrichosis-5, also known as Marie Unna hereditary hypotrichosis (Zhang et al. 2012). To the best of our knowledge, no defects associated with mutations of EPS8L1 have been reported yet. To get a better understanding of EPS8L1, we here determined the precise expression pattern of EPS8L1 within the skin and its evolutionary conservation among mammals.

The present study shows that the distribution of the EPS8L1 protein occurs in the granular and transitional layer, while the protein is no longer detectable in the external part of the corneous layers of the epidermis, in the basal and suprabasal layers in most mammalian epidermises here analyzed. The distribution of labeling indicates that the EPS8L1 protein is temporarily present in the cytoplasm of terminal differentiating keratinocytes but is not associated to pro-filaggrin/filaggrin containing F-granules (Steven et al. 1990; Ishida-Yamamoto et al. 2000, 2018). EPS8L1 immunolabeling appears of lower intensity in comparison to that for involucrin. In general, however, EPS8L1 immunolabeling resembles that of two of the main proteins involved in barrier formation, involucrin and loricrin, as described for mouse, rat, and humans (Warhol et al. 1985; Steven et al 1990; Ishida-Yamamoto et al. 2000, 2018; Alibardi 2009), and also observed to localized in similar areas of monotreme and marsupial epidermis (Alibardi and Maderson 2003; Alibardi 2010, 2012). This information suggests that the EPS8L1 protein has a general role in the formation of the epidermal barrier, in association with the above two major corneous proteins. Interestingly, knockout of loricrin causes an increase of EPS8L1 in cornified envelopes of mouse epidermis, as determined by mass spectrometry-based proteomic analysis (Rice et al. 2016). Detailed observations under TEM indicated that the cytoplasmic labeling in the human epidermis tends to intensify along cell junctions and perimeter of keratinocytes in the stratum transitional and lower corneous, when keratinocytes become fully mature as corneocytes. The immunolocalization is lost in mature corneocytes and in those that are desquamating where rare gold particles are seen with random distribution. EPS8L1 is expressed in cells that also contains transglutaminases (Sachslehner et al. 2023) and contains several amino acid sites for isopeptide bonding but only further studies will be able to show a direct incorporation of this protein into the corneous layer. However, as EPS8L1 is detected by proteomic analysis in the stratum corneum of both mice (Rice et al. 2016) and humans (Karim et al. 2019; Sølberg et al. 2023), it is likely that EPS8L1 is incorporated into cornified envelopes and its epitope is masked after full cornification.

The immunolocalization of the EPS8L1 protein in the IRS of mammalian hairs, which represents a shedding layer for the emergence of the hair shaft on the epidermal surface, further supports a role for this protein in the formation of the follicular hair barrier, impeding the penetration of chemicals and microbes inside the follicle and the hair bulb. It is known that in both placental granular and transitional keratinocytes of the epidermis and in the Henle-Huxley cells of the IRS of the hair follicle also the polarization of tight junctions contribute to the formation of these epidermal and hair follicle barriers (Mathes et al. 2016; Gorzelanny et al. 2020).

Aside from mammalian epidermis, the epidermis of lizard scales has been reported to contain EPS8L1 in maturing keratinocytes of specific layers and indicated as clear and alpha-layers (Alibardi 2023). The keratinocytes formed in these two layers for some aspects resemble those of the granular and transitional layers of mammalian epidermis. Also, in lizard epidermis the EPS8L1 protein localization appears related to the formation of an epidermal barrier that is formed beneath the mature corneous layer before it is shed as a molt (Alibardi 2023). Our comparative genomics results showed that EPS8L1 is absent in birds, suggesting that it is not essential for the formation of the epidermal barrier in amniotes in general. However, it is currently unknown whether another protein substitutes for EPS8L1 in avian epidermis.

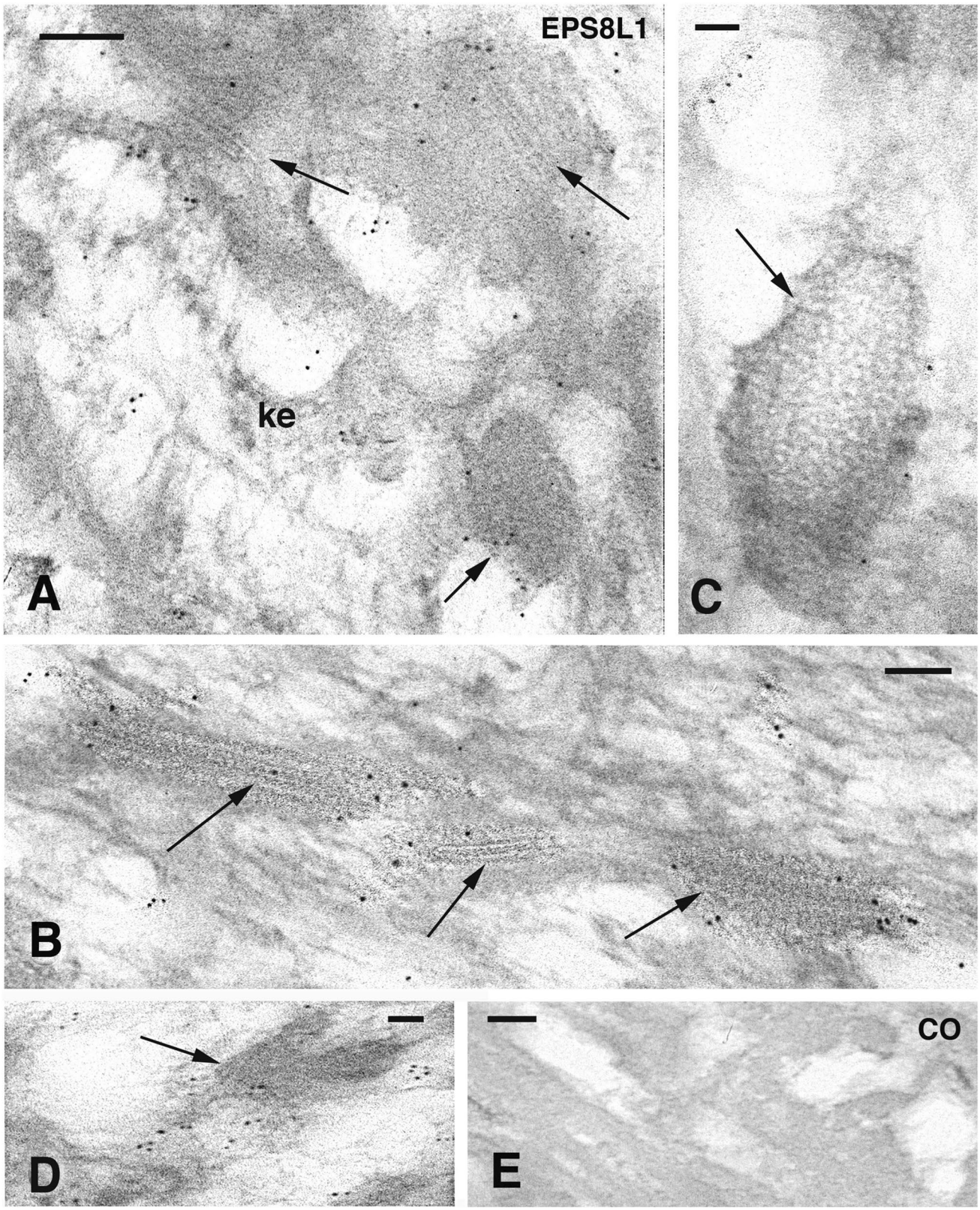

Fig. 8 TEM immunogold view of human epidermis for EPS8L1. **A** Detail of the sparsely labeled cytoplasm with keratin (ke) of granular cell. Desmosomal remnants associated with weakly labeled dense corneous material (arrows) are seen. Bar, 200 nm. **B** Desmosomal remnants (arrows) in granular cells with associated labeling. Bar, 200 nm. **C** Unlabeled F-keratohyaline granule (arrow). Bar, 100 nm. **D** Detail of the labeling associated to a denser corneous material (arrow) in a transitional cell. Bar, 100 nm. **E** Immunonegative cytoplasmic detail of a transitional cell in a control section (co). Bar, 200 nm

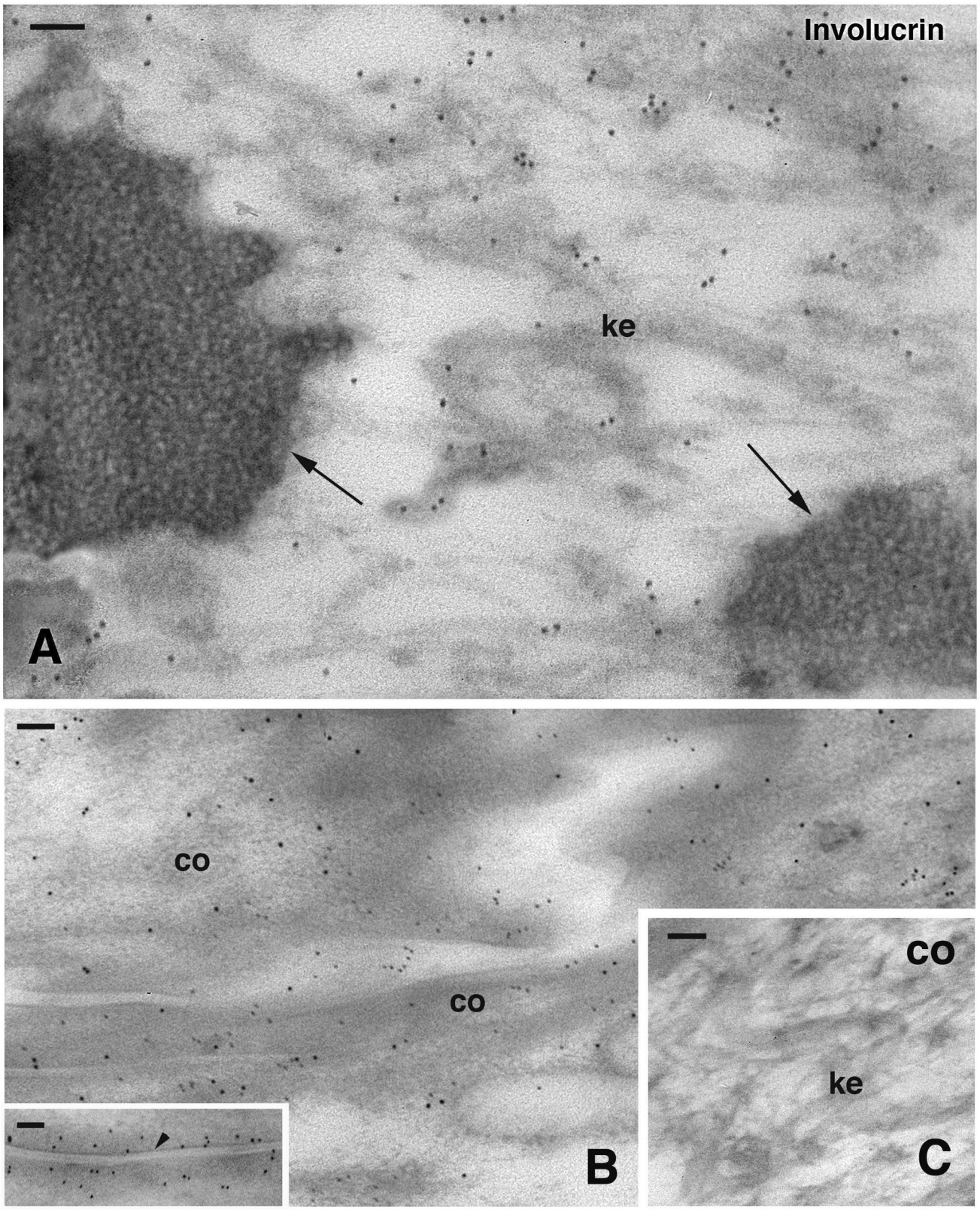

Fig. 9 Transmission electron microscopic immunogold labeling for involucrin. **A** Detail on the cytoplsma of a cell of the granular layer showing the prevalent association of gold particles with keratin bundles (ke) but not on keratohyaline granules (arrows). Bar, 100 nm. **B** Evenly distributed immunolabeling in transitional and lower corneous layer cells (co). Bar, 100 nm. The inset (bar, 100 nm) details on some labeling along the periphery of corneocytes with the (forming) cell corneous envelope (arrowhead). **C** Immunonegative cytoplasm and keratin bundles (ke) of granular cell. Bar, 100 nm

In conclusion, the present comparative immunolabeling study suggests that EPS8L1 is associated with barrier formation in mammalian epidermis and hair follicles, but its specific biochemical role remains to be clarified.

Acknowledgements We thank Maria Buchberger, Bahar Golabi, Dragan Copic, and Erwin Tschachler (Medical University of Vienna) for helpful discussions. The study was partly self-supported (LA). This paper is dedicated to my (LA) beloved father-in law, Bruno, who was the closer oldest friend that I ever had.

Declarations

Competing Interests The authors declare no competing interests in the present manuscript.

References

Alibardi L (2004a) Fine structure and immunocytochemistry of monotreme hairs with emphasis on the inner root sheath and trichohyaline-based cornification during hair evolution. J Morphol 261:345–363

Alibardi L (2004b) Fine structure of marsupial hairs with emphasis on trichohyalin and the structure of the inner root sheath. J Morphol 261:390–402

Alibardi L (2006) Ultrastructure of bat (*Pipistrellus kuhlii*) epidermis with emphasis on terminal differentiation of corneocytes. Zool Res 27:86–93

Alibardi L (2009) Review: embryonic keratinization in vertebrates in relation to land colonization. Acta Zool (stockolm) 90:1–17

Alibardi L (2010) The ultrastructural immunolocalization of loricrin in the hairy epidermis of the platypus (*Ornithorhynchus anatinus*, Monotremata) indicates it contributes to the formation of the cell corneous envelope. Belg J Zool 140:59–64

Alibardi L (2012) Ultrastructural pattern of loricrin localization in the epidermis of the red kangaroo *Macropus rufus* (Marsupialia, Mammalia) in relation to the formation of the stratum corneum in mammalian epidermis. Ital J Zool 79:69–76

Alibardi L (2023) Immunolocalization of Pglyrp3 and Eps8l1 proteins in the regenerating lizard epidermis indicates they contribute to epidermal barrier formation. Zoology 157:126080

Alibardi L, Maderson PFA (2003) Distribution of keratins and associated proteins in the epidermis of monotremes, marsupial and placental mammals. J Morphol 258:49–66

Alibardi L, Dockal M, Reinisch C, Tschachler E, Eckart L (2004) Ultrastructural localization of caspase-14 in human epidermis. J Histochem Cytochem 52:1561–1574

Alibardi L, Tschachler E, Eckhart L (2005) Distribution of caspase-14 in epidermis and hair follicles is evolutionary conserved among mammals. Anat Rec 286A:962–973

Amberg N, Sotiropoulou PA, Heller G, Lichtenberger BM, Holcmann M, Camurdanoglu B, Baykuscheva-Gentscheva T, Blanpain C, Sibilia M (2019) EGFR controls hair shaft differentiation in a p53-independent manner. IScience 15:243–256

Barresi C, Rossiter H, Buchberger M, Pammer J, Sukseree S, Sibilia M, Tschachler E, Eckhart L (2022) Inactivation of autophagy in keratinocytes reduces tumor growth in mouse models of epithelial skin cancer. Cells 11:3691

Eckhart L, Zeeuwen PLJM (2018) The skin barrier: Epidermis vs environment. Exp Dermatol 27:805–806

Eckhart L, Uthman A, Sipos W, Tschachler E (2006) Genome sequence comparison reveals independent inactivation of the caspase-15 gene in different evolutionary lineages of mammals. Mol Biol Evol 23:2081–2089

Eckhart L, Schmidt M, Mildner M, Mlitz V, Abtin A, Ballaun C, Fischer H, Mrass P, Tschachler E (2008) Histidase expression in human epidermal keratinocytes: regulation by differentiation status and all-trans retinoic acid. J Dermatol Sci 50:209–215

Edqvist PH, Fagerberg L, Hallström BM, Danielsson A, Edlund K, Uhlén M, Pontén F (2015) Expression of human skin-specific genes defined by transcriptomics and antibody-based profiling. J Histochem Cytochem 63:129–141

Elias PM, Choi EH (2005) Review. Interactions among stratum corneum defensive functions. Exp Dermatol 14:719–726

Frittoli E, Matteoli G, Palamidessi A, Mazzini E, Maddaluno L, Disanza A, Yang C, Svitkina T, Rescigno M, Scita G (2011) The signaling adaptor Eps8 is an essential actin capping protein for dendritic cell migration. Immunity 35:388–399

Furness DN, Johnson SL, Manor U, Rüttiger L, Tocchetti A, Offenhauser N, Olt J, Goodyear RJ, Vijayakumar S, Dai Y, Hackney CM, Franz C, Di Fiore PP, Masetto S, Jones SM, Knipper M, Holley MC, Richardson GP, Kachar B, Marcotti W (2013) Progressive hearing loss and gradual deterioration of sensory hair bundles in the ears of mice lacking the actin-binding protein Eps8L2. Proc Natl Acad Sci U S A 110:13898–13903

Giampietro C, Disanza A, Bravi L, Barrios-Rodiles M, Corada M, Frittoli E, Savorani C, Lampugnani MG, Boggetti B, Niessen C, Wrana JL, Scita G, Dejana E (2015) The actin-binding protein EPS8 binds VE-cadherin and modulates YAP localization and signaling. J Cell Biol 211:1177–1192

Gorzelanny C, Mess C, Schneider SW, Huck V, Brandner JM (2020) Skin barriers in dermal drug delivery: which barriers have to be overcome and how can we measure them? Pharmaceutics 12:684

Green KJ, Niessen CM, Rübsam M, Perez White BE, Broussard JA (2022) The desmosome-keratin scaffold integrates ErbB family and mechanical signaling to polarize epidermal structure and function. Front Cell Dev Biol 10:903696

Gulati N, Krueger JG, Suárez-Fariñas M, Mitsui H (2013) Creation of differentiation-specific genomic maps of human epidermis through laser capture microdissection. J Invest Dermatol 133:2640–2642

Ishida-Yamamoto A, Takahashi H, Iizuka H (2000) Immunoelectron microscopy links molecules and morphology in the studies of keratinization. Eur J Dermatol 10:429–435

Ishida-Yamamoto A, Igawa S, Kishibe M (2018) Molecular basis of the skin barrier structures revealed by electron microscopy. Exp Dermatol 27:841–846

Kalinin AE, Kajava AV, Steinert PM (2002) Epithelial barrier function: assembly and structural features of the cornified cell envelope. BioEssays 24:789–800

Kalinina P, Vorstandlechner V, Buchberger M, Eckhart L, Lengauer B, Golabi B, Laggner M, Hiess M, Sterniczky B, Födinger D, Petrova E, Elbe-Bürger A, Beer L, Hovnanian A, Tschachler E, Mildner M (2021) The whey acidic protein WFDC12 is specifically expressed in terminally differentiated keratinocytes and regulates epidermal serine protease activity. J Invest Dermatol 141:1198–1206

Karim N, Phinney BS, Salemi M, Wu PW, Naeem M, Rice RH (2019) Human stratum corneum proteomics reveals cross-linking of a broad spectrum of proteins in cornified envelopes. Exp Dermatol 28:618–622

Lanzetti L, Rybin V, Malabarba MG, Christoforidis S, Scita G, Zerial M, Di Fiore PP (2000) The Eps8 protein coordinates

EGF receptor signalling through Rac and trafficking through Rab5. Nature 408:374–377

Lichtenberger BM, Gerber PA, Holcmann M, Buhren BA, Amberg N, Smolle V, Schrumpf H, Boelke E, Ansari P, Mackenzie C, Wollenberg A, Kislat A, Fischer JW, Röck K, Harder J, Schröder JM, Homey B, Sibilia M (2013) Epidermal EGFR controls cutaneous host defense and prevents inflammation. Sci Transl Med 5:199ra111

Mathes C, Brandner JM, Laue M, Raesch SS, Hansen S, Failla AV, Vidal S, Moll I, Schaefer UF, Lehr CM (2016) Tight junctions form a barrier in porcine hair follicles. Eur J Cell Biol 95:89–99

Matsui T, Amagai M (2015) Dissecting the formation, structure and barrier function of the stratum corneum. Int Immunol 27:269–280

Matsui T, Kadono-Maekubo N, Suzuki Y, Furuichi Y, Shiraga K, Sasaki H, Ishida A, Takahashi S, Okada T, Toyooka K, Sharif J, Abe T, Kiyonari H, Tominaga M, Miyawaki A, Amagai MA (2021) Unique mode of keratinocyte death requires intracellular acidification. Proc Natl Acad Sci USA 118:e2020722118

Menon GK, Ghadially R, Williams ML, Elias PM (1992) Lamellar bodies as delivery systems of hydrolytic enzymes: implications for normal and abnormal desquamation. Br J Dermatol 126:337–345

Offenhauser N, Borgonovo A, Disanza A, Romano P, Ponzanelli I, Iannolo G, Di Fiore PP, Scita G (2004) The eps8 family of proteins links growth factors stimulation to actin reorganization generating functional redundancy in the Ras/Rac pathway. Mol Biol Cell 15:91–98

Rawlings AV, Scott IR, Harding CR, Bowser PA (1994) Stratum corneum moisturization at the molecular level. J Invest Dermatol 103:731–740

Rice RH, Durbin-Johnson BP, Ishitsuka Y, Salemi M, Phinney BS, Rocke DM, Roop DR (2016) Proteomic analysis of loricrin knockout mouse epidermis. J Proteome Res 15:2560–2566

Rübsam M, Mertz AF, Kubo A, Marg S, Jüngst C, Goranci-Buzhala G, Schauss AC, Horsley V, Dufresne ER, Moser M, Ziegler W, Amagai M, Wickström SA, Niessen CM (2017) E-cadherin integrates mechanotransduction and EGFR signaling to control junctional tissue polarization and tight junction positioning. Nat Commun 8:1250

Sachslehner AP, Surbeck M, Golabi M, Geiselhofer M, Jager K, Hess C, Kuchler U, Gruber R, Eckhart L (2023) Transglutaminase activity is conserved in stratified epithelia and skin appendages of mammals and birds. Int J Mol Sci 24:2193

Scala C, Cenacchi G, Ferrari C, Pasquinelli G, Preda P, Manara G (1992) A new acrylic resin formulation: a useful tool for histological, ultrastructural, and immunocytochemical investigations. J Histochem Cytochem 40:1799–1804

Sokolov VE (1982) Mammalian skin. University of California Press, Berkley-Los Angeles-New York

Sølberg JBK, Quaade AS, Drici L, Sulek K, Ulrich NH, Løvendorf MB, Thyssen JP, Mann M, Dyring-Andersen B, Johansen JD (2023) The proteome of hand eczema assessed by tape stripping. J Invest Dermatol 143:1559–1568

Steven AC, Bisher ME, Roop DR, Steinert PM (1990) Biosynthetic pathways of filaggrin and loricrin-two major proteins expressed by terminally differentiated epidermal keratinocytes. J Struct Biol 104:150–162

Tocchetti A, Confalonieri S, Scita G, Di Fiore PP, Betsholtz C (2003) In silico analysis of the EPS8 gene family: genomic organization, expression profile, and protein structure. Genomics 81:234–244

Warhol MJ, Roth J, Lucocq JM, Pinkus GS, Rice RH (1985) Immunoultrastructural localization of involucrin in squamous epithelium and cultured keratinocytes. J Histochem Cytochem 33:141–149

Wu Z, Hansmann B, Meyer-Hoffert U, Gläser R, Schröder JM (2009) Molecular identification and expression analysis of filaggrin-2, a member of the S100 fused-type protein family. PLoS ONE 4:e5227

Zampini V, Rüttiger L, Johnson SL, Franz C, Furness DN, Waldhaus J, Xiong H, Hackney CM, Holley MC, Offenhauser N, Di Fiore PP, Knipper M, Masetto S, Marcotti W (2011) Eps8 regulates hair bundle length and functional maturation of mammalian auditory hair cells. PLoS Biol 9:e1001048

Zhang X, Guo BR, Cai LQ, Jiang T, Sun LD, Cui Y, Hu JC, Zhu J, Chen G, Tang XF, Sun GQ, Tang HY, Liu Y, Li M, Li QB, Cheng H, Gao M, Li P, Yang X, Zuo XB, Zheng XD, Wang PG, Wang J, Wang J, Liu JJ, Yang S, Li YR, Zhang XJ (2012) Exome sequencing identified a missense mutation of EPS8L3 in Marie Unna hereditary hypotrichosis. J Med Genet 12:727–730